Neurobiology of Aging 76 (2019) 106–114

Contents lists available at ScienceDirect

Neurobiology of Aging

journal homepage: www.elsevier.com/locate/neuaging

Age-related cortical signatures of human sleep electroencephalography

Véronique Latreille [a,b], Malo Gaubert [a,c], Jonathan Dubé [a,b], Jean-Marc Lina [a,d], Jean-François Gagnon [a,c], Julie Carrier [a,b,*]

[a] Centre for Advanced Research in Sleep Medicine, Hôpital du Sacré-Coeur de Montréal, Montreal, Quebec, Canada
[b] Department of Psychology, Université de Montréal, Montreal, Quebec, Canada
[c] Department of Psychology, Université du Québec à Montréal, Montreal Quebec, Canada
[d] Department of Electrical Engineering, École de Technologie Supérieure, Montreal, Quebec, Canada

ARTICLE INFO

Article history:
Received 9 May 2018
Received in revised form 17 December 2018
Accepted 27 December 2018
Available online 6 January 2019

Keywords:
Aging
Cortical thickness
Sleep electroencephalography

ABSTRACT

Accumulating evidence demonstrates a direct relationship between impaired neural integrity and disrupted sleep physiology in normal and pathological aging. However, previous work has focus almost exclusively on nonrapid eye movement sleep electroencephalography as a proxy of cortical integrity with aging. Whether this relationship holds true for rapid eye movement sleep electroencephalography is unknown. Our results show that age-related reduction in low-frequency delta activity during both rapid eye movement and nonrapid eye movement sleep was statistically mediated by the thinning of the medial frontal and anterior cingulate cortices. These findings (1) support the potential role of the medial frontal and cingulate cortices, major hubs of the human brain, in synchronizing neuronal assemblies during sleep, and (2) suggest that, with age, a reduction in cortical integrity within this frontal network mediates the loss of delta power during sleep. Further work will determine whether cortical thinning and delta loss may interact and contribute to cognitive decline with aging.

1. Introduction

The sleep electroencephalographic (EEG) may provide precious insights about the integrity of the underlying neuronal networks. Indeed, in health and disease, changes in neuronal structure have direct impacts on sleep EEG physiology (Dube et al., 2015; Mander et al., 2013, 2016). It is now well established that sleep undergoes major changes with normal aging (Mander et al., 2017). Accumulating evidence demonstrates that nonrapid eye movement (NREM) sleep may be particularly affected by the aging process. Indeed, slow waves and sleep spindles, as well as their corresponding EEG frequency components, delta (<4 Hz) and sigma (~11–16 Hz) activity, decrease substantially with age, mostly in anterior cortical regions (Carrier et al., 2011; Landolt and Borbély, 2001; Martin et al., 2013). The precise mechanisms by which aging disrupts sleep EEG rhythms are not fully understood, but recent evidence suggests that age-related brain structural changes may be involved (Dube et al., 2015; Mander et al., 2013). Particularly, age-related cortical thinning and reduced gray matter volume in frontal and prefrontal areas statistically explain the effects of age on NREM sleep slow-wave activity (Dube et al., 2015; Mander et al., 2013). That is, structural brain changes throughout adulthood constitute an important mechanism by which age impacts sleep slow waves.

Whether REM sleep EEG may also serve as a proxy of cortical integrity in normal aging is undetermined. Yet, age has a similar influence on EEG patterns of both NREM and REM sleep: delta activity is reduced with advancing age, whereas higher frequencies start to permeate the EEG (Carrier et al., 2011; Landolt and Borbély, 2001; Luca et al., 2015). Moreover, although NREM and REM sleep EEG rhythms differ as regard to their underlying neurophysiological mechanisms (Krishnan et al., 2016), they share common brain substrates. Studies using positron emission tomography imaging in healthy young adults have demonstrated that common brain regions are either similarly activated or deactivated during NREM and REM sleep (i.e., amygdala, prefrontal cortex, supramarginal, and precuneus gyri), or they show state-dependent, opposite patterns (i.e., thalamus, brainstem pontine tegmentum, and anterior cingulate cortex) (Hofle et al., 1997; Maquet, 2000; Maquet et al., 1996, 1997; Nofzinger et al., 2002). Moreover, a recent high-density EEG study revealed that some regions (mostly central and occipital scalp derivations) displayed high delta power during both REM and NREM sleep (Baird et al., 2018). Taken altogether, it may be

* Corresponding author at: Centre for Advanced Research in Sleep Medicine, Hôpital du Sacré-Coeur de Montréal, 5400 West Gouin Boulevard, Montreal, Quebec H4J 1C5, Canada. Tel.: +1 514 338 2222 ext. 3124; fax: +1 514 338 2531.
E-mail address: julie.carrier.1@umontreal.ca (J. Carrier).

0197-4580/$ – see front matter © 2019 Elsevier Inc. All rights reserved.
https://doi.org/10.1016/j.neurobiolaging.2018.12.012

postulated that the reduction of delta activity during NREM and REM sleep with aging can be accounted for by common cortical-subcortical brain mechanisms. Moreover, because we know that several subcortical structures such as the thalamus, hippocampus, and putamen are involved in both REM and NREM sleep (Dang-Vu et al., 2005; Maquet et al., 1996, 1997), and that they are not spared by normal aging (Fjell and Walhovd, 2010; Goodro et al., 2012; Long et al., 2012), their involvement in modifying sleep EEG with age should be investigated.

Using cortical thickness and subcortical volumetry in a cohort of young and older healthy adults, we investigated (1) the cortical-subcortical signature of REM sleep EEG in adults; (2) whether the age-related differences in low-frequency EEG activity during REM sleep were associated with lower frontal cortical thickness and reduced thalamic and hippocampal volumes; and (3) if the reduction in low-frequency EEG activity during both REM and NREM sleep can be accounted for by common cerebral substrates.

2. Materials and methods

2.1. Participants

Sixty healthy subjects, including 30 young adults (16 men; 22–32 years; age, mean ± SD = 22.8 ± 2.8 years) and 30 older adults (12 men and 18 women; 50–69 years old; age, mean ± SD = 59.6 ± 5.6) participated in this study. Participants were recruited as part of a prospective study on sleep and neuroimaging in healthy aging. A subset of this cohort of subjects was included in a previous study (Dube et al., 2015). All participants were screened for various potential health-related confounds, including any sleep disorders, cognitive complaints, reported sleep times of <7 hours or >9 hours, medications known to affect the sleep-wake cycle, and history of neurological or psychiatric conditions. They all underwent an adaptation and screening overnight polysomnography (PSG), followed by a second full-night PSG which was used for data analysis. Participants were instructed to keep a regular sleep-wake cycle (±30 minutes) based on their habitual sleep-wake schedule. All participants kept a sleep agenda the week before the PSG recordings and the regularity of their sleep-wake cycle was confirmed with actigraphy. Subjects were excluded if they scored higher than 13 on the Beck Depression Inventory, Second Edition (Beck et al., 1961). Moreover, all participants underwent a complete neuropsychological assessment to ensure their cognition was unimpaired. One older male subject was excluded from the analysis because of mild cognitive deficits on the neuropsychological examination (American Psychiatric Association, 2013). Therefore, a total of 59 subjects were included in the study, of which 29 were older cognitively normal adults (11 men; age, mean ± SD = 59.5 ± 5.6 years). The study was approved by the research ethics board of the Regroupement Neuroimagerie Québec. All subjects signed an informed consent form and received monetary compensation for participating in the study.

2.2. Polysomnographic recording

The PSG montage included 20 EEG leads (International 10–20 system) in reference to linked ears with a 10 kΩ resistance, a bilateral electro-oculogram, and submental electromyographic recordings. Subjects with an apnea-hypopnea index >10 or periodic leg movement index >10 were excluded from the study. PSG was recorded with a Grass polygraph (amplifier gain 10,000; bandpass 0.3–100 Hz), and signals were digitized at a sampling rate of 256 Hz using the Harmonie software (Stellate Systems, Montreal, Canada). Sleep stages were visually scored on 30-second epochs according to standard criteria (Iber et al., 2007). PSG variables included bed and wake times, total sleep time, time spent in bed, sleep efficiency and latency, REM sleep latency, wake after sleep onset (WASO), number of awakenings, and sleep stage percentages.

2.3. Sleep EEG analysis

Quantitative EEG analyses were performed over averaged derivations yielding 5 regions: frontal (Fp1, Fp2, F3, F4, F7, F8, Fz), central (C3, C4, Cz), temporal (T3, T4, T5, T6), parietal (P3, P4, Pz), and occipital (O1, O2, Oz). Spectral analyses of REM and NREM sleep were computed using fast Fourier transforms (with cosine tapering) on artifact-free EEG sections (Bolduc et al., 2003; Brayet et al., 2014; Latreille et al., 2016; Léveillé et al., 2010; Morisson et al., 1998; Petit et al., 1993). For REM sleep analyses, EEG sections of at least 2 seconds duration, free of eye movements (tonic REM sleep), arousals, or artifacts were visually sampled across the second, third, and fourth REM periods, when available. In all subjects, REM sleep EEG data were sampled from at least 2 REM epochs. A minimum of 60 seconds of artifact-free REM sleep epochs were required per subject (range, young adults = 70–527 seconds, older adults = 64–384 seconds). For NREM sleep analyses (stages N2 and N3), artifacts were detected automatically and visually, and then eliminated before analysis (Brunner et al., 1996). Epochs contaminated by artifacts were considered as missing data to maintain sleep continuity. Six 5-second spectral epochs were averaged to preserve the correspondence with the 30-second sleep-scoring windows (range, young adults = 150–334 minutes, older adults = 160–341 minutes). To account for potential individual differences in absolute spectral power, REM and NREM sleep spectral values in each classically defined frequency bands were normalized (separately) to total spectral power (0.5–32 Hz). Relative spectral power in the delta (REM: 0.5–4 Hz; NREM: 0.6–4 Hz), theta (4–8 Hz), alpha (8–13 Hz), and beta (13–32 Hz) frequency ranges were computed across 5 cortical areas (frontal, central, temporal, parietal, and occipital). Absolute spectral power was also computed for the same frequency bands and EEG derivations (see Supplementary Fig. 2 for results).

2.4. MRI acquisition

All participants were scanned at the Functional Neuroimaging Unit (Montreal, Canada) using a 3 Tesla MAGNETOM TrioTIM scanner (12 channels) manufactured by Siemens (Munich, Germany). The MRI scans were performed within 1 month from the PSG recordings. The T1 magnetization-prepared rapid acquisition with gradient-echo (MPRAGE) sequence was acquired using the following parameters: TR = 2.3 seconds, TE = 2.91 ms, flip angle = 9°, matrix = 256 × 240 mm, in-plane resolution = 1 × 1 mm^2.

2.5. Cortical thickness analysis

Cortical thickness was measured in all participants using version 6.0 of the FreeSurfer processing pipeline (Laboratory for Computational Neuroimaging, Athinoula A. Martinos Center for Biomedical Imaging, Boston, USA), a widely used image analysis suite ([Fischl and Dale, 2000] for cortical thickness measurement algorithms). Cortical thickness represents the distance between gray and white matter surface. A detailed review of each processing steps can be found online (http://freesurfer.net/fswiki/FreeSurferMethodsCitation). Visual inspection of images at each step of the processing pipeline was carefully carried out by the same operator (M.G.) to ensure accurate normalization, skull stripping, white/pial surface generation, and tissue classifications. All images were smoothed with a 15-mm full width at half maximum surface-based kernel to improve signal-to-noise ratio and minimize the impact of registration errors. Cortical

regions were labeled according to the Desikan-Killiany atlas (Desikan et al., 2006).

2.6. Subcortical volumetry

A shape-based algorithm (Patenaude et al., 2011) implemented in FSL FIRST 5.0 (Oxford Centre for Functional MRI of the Brain, Oxford, UK) was used to calculate global volumes (expressed in cubic millimeters) of 7 bihemispheric subcortical structures: thalamus, caudate nucleus, putamen, pallidum, hippocampus, amygdala, and nucleus accumbens. To reduce interindividual head size differences, each subcortical structure was adjusted by multiplying its volume by the estimated FSL SIENA scaling factor.

2.7. Statistical analysis

2.7.1. Age differences in demographic and sleep data

Independent sample *t*-tests, Mann-Whitney *U* tests, or Pearson's χ^2 tests were performed to compare demographic and PSG data in young and older adults. The effects of age on sleep EEG spectral power (REM and NREM sleep) were examined using analyses of covariance (ANCOVAs) with 2 groups, one repeated measure (5 regions), and sex as a covariate. *p*-Values were adjusted for sphericity with the Huynh-Feldt correction for repeated measures with more than 2 levels, but original degrees of freedom are reported. Mean comparison analyses were performed with Tukey's post hoc tests and simple effect analyses were run to decompose significant interactions.

2.7.2. Age-related cortical and subcortical differences

To assess the effects of age on cortical integrity, linear regressions between age and whole-brain cortical thickness were performed in all subjects, with sex as a covariate. Statistical surface maps were created using a vertexwise statistical threshold of $p < 0.01$. Corrections for multiple comparisons were performed using a Monte Carlo clusterwise simulation, limited to positive or negative clusters, and set at $p < 0.001$. Age effects on subcortical volumes were examined in all subjects using linear regressions, with sex as a covariate. *p*-Values were adjusted for the false discovery rate (FDR) (Benjamini and Hochberg, 1995), and corrected *p*-thresholds ($p' < 0.05$) are reported.

2.7.3. Relationships between gray matter and sleep EEG

As a next step, we performed linear regressions (controlling for age and sex) to test the relationship between sleep EEG spectral power and cortical integrity. Statistical surface maps were created using a vertexwise statistical threshold of $p < 0.01$. Corrections for multiple comparisons were performed using a Monte Carlo clusterwise simulation, limited to positive or negative clusters, and set at $p < 0.05$. Right and left hemispheres were tested separately. Relationships between subcortical volumes and sleep EEG were assessed using regression models, with age and sex as covariates. *p*-Values were adjusted for the FDR ($p' < 0.05$).

2.7.4. Mediation modeling

Simple mediation analyses were performed to test for indirect effects, namely whether the effects of age on cortical gray matter integrity may statistically explain some of the differences observed in sleep EEG with aging (Supplementary Fig. 1). We included all the sleep EEG variables that showed significant age effects (Fig. 1). We first performed conjunction analyses to identify cortical regions that were associated with both age (path a) and sleep EEG (path b, controlling for age). To do so, we computed an independent age effect statistical surface map (with sex as a covariate) using a vertexwise statistical threshold of $p < 0.05$, and corrected results at $p < 0.001$ using a Monte Carlo simulation. We then isolated each cluster present in the former contrast map (age effects) with the intersecting sleep EEG contrast map (while controlling for age and sex), and corrected results at $p < 0.05$ using a Monte Carlo simulation. For each of these conjunction clusters, mean cortical thickness for all subjects was extracted in the

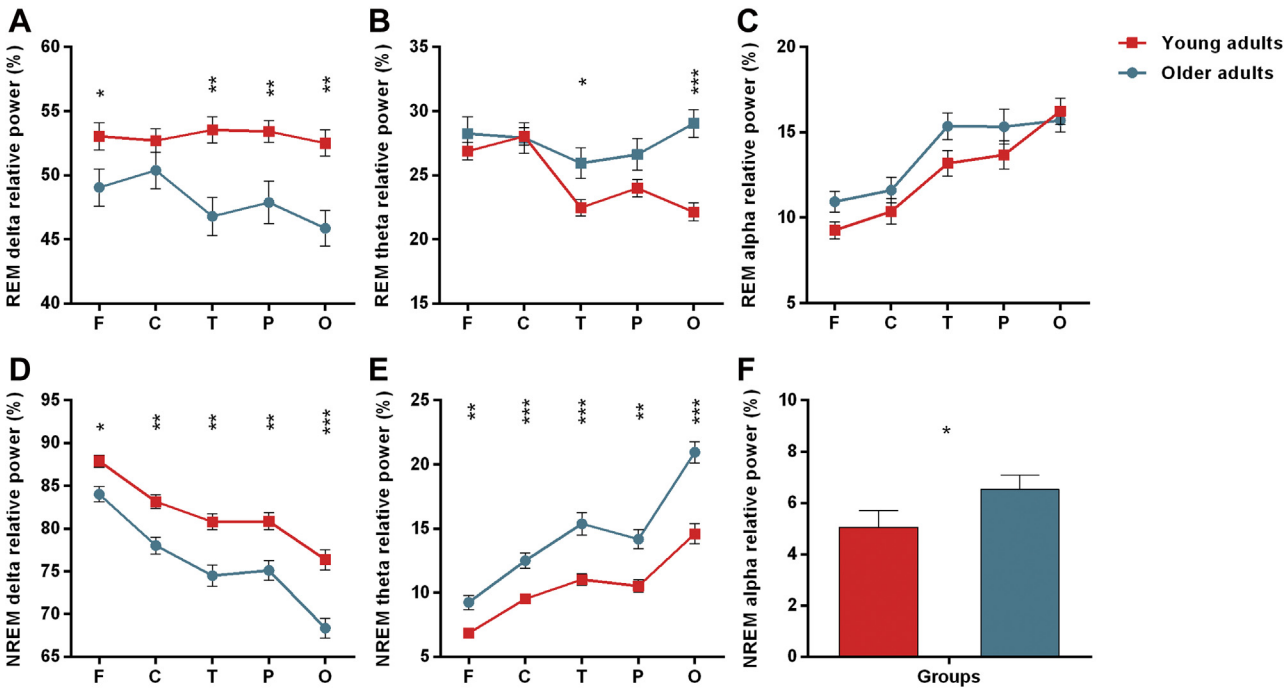

Fig. 1. Age-related topographical changes in REM and NREM sleep EEG activity. Relative spectral power in REM (top panel) and NREM (bottom panel) frequency bands for each region in young (red) and older adults (blue): (A) REM sleep delta, (B) REM sleep theta, (C) REM sleep alpha, (D) NREM sleep delta, (E) NREM sleep theta, and (F) NREM sleep alpha. Contrast analyses: $^{*}p < 0.05$; $^{**}p < 0.001$; $^{***}p < 0.0001$. Error bars indicate SEM. Abbreviations: REM, rapid eye movement; NREM, nonrapid eye movement; EEG, electroencephalography. (For interpretation of the references to color in this figure legend, the reader is referred to the Web version of this article.)

native space. These extracted clusters were then independently used in the statistical models testing mediation.

To test the hypothesis that aging influences sleep EEG (path c) through an initial effect on gray matter integrity (path a), which in turn will cause changes in sleep EEG (path b), simple mediation analyses were performed using established methods (PROCESS macro, version 2.16 for SPSS) (Hayes, 2013). Mediation occurs when a predictor influences a dependent variable through a third mediator variable (indirect effect). Indirect effects were examined using a percentile bootstrap (95% confidence interval) based on 10,000 bootstrap samples, and effects were considered significant ($p < 0.05$) when the bootstrapped confidence interval did not include zero. Sex was included as a covariate in all mediation models. Unstandardized regression coefficients and partially standardized effect sizes are reported.

3. Results

3.1. Age effects on sleep macroarchitecture

As expected, sleep macroarchitecture was globally modified in older adults as compared with younger individuals (see Supplementary Table 1). Older adults slept less and more poorly than younger adults. They also spent more time in lighter sleep stages, paralleled by a reduced time spent in deeper sleep stages.

3.2. Age-related sleep EEG differences

3.2.1. REM sleep

Compared with younger adults, older adults showed lower overall relative delta power, but this difference was more prominent in temporal, parietal, and occipital regions (group*region interaction: $F(4,224) = 6.1$; $p = 0.0006$; Fig. 1A). Conversely, older individuals had significantly higher theta power as compared with younger participants in temporal and occipital regions (group*region interaction: $F(4,224) = 18.7$; $p < 0.00001$; Fig. 1B). Finally, alpha power tended to be higher in older adults as compared with younger subjects in the frontal ($p = 0.05$) region (group*region interaction: $F(4,224) = 3.5$; $p = 0.02$; Fig. 1C). No significant age-related effects were observed for beta power.

3.2.2. NREM sleep

We found comparable age-related patterns in NREM sleep as in REM sleep: older adults showed lower relative delta power (group*region interaction: $F(4,224) = 6.0$; $p = 0.002$; Fig. 1D) as well as higher relative theta (group*region interaction: $F(4,224) = 10.5$; $p = 0.00005$; Fig. 1E) and alpha power (group effect: $F(1,56) = 6.7$; $p = 0.01$; Fig. 1F), compared with younger adults. Age-related effects on delta and theta power were more prominent in the posterior regions, whereas age effects on alpha frequencies were similar across the scalp (no group*region interaction). No significant age effects were observed for beta power in NREM sleep. Overall, our results indicate marked age-related differences in REM and NREM sleep relative delta activity and this is consistent with prior studies (Landolt and Borbély, 2001; Luca et al., 2015).

3.3. Age-related gray matter differences

3.3.1. Cortical thickness

As expected, and consistent with the literature (Lemaitre et al., 2012; Shaw et al., 2016), older age was associated with widespread cortical thinning (Table 1). More specifically, we found significant age-related reductions in cortical thickness in the left precentral gyrus (extending to the orbitofrontal cortices, pars triangularis, opercularis and orbitalis gyri, cingulate and insular cortices), the left inferior temporal gyrus, the left fusiform gyrus, the right superior parietal lobule (extending to the inferior parietal, precuneus, cuneus, and lingual cortices), and the right postcentral gyrus (extending to the superior parietal cortex; all controlling for sex, $p < 0.001$ corrected using a Monte Carlo simulation). No significant increase in cortical thickness was found with advancing age.

3.3.2. Subcortical volumes

Consistent with prior reports (Fjell and Walhovd, 2010; Goodro et al., 2012) and as delineated in Table 1, age was associated with reduced subcortical gray matter volume bilaterally in the thalami, caudate nuclei, putamina, and accumbens nuclei (controlling for sex $p' < 0.05$ FDR-corrected). No significant age effect was found for the hippocampi, amygdalae, and globus pallidi.

3.4. Relationship between gray matter integrity and sleep EEG

3.4.1. REM sleep

In all subjects (independent of age and sex), greater cortical thickness in the superior frontal gyrus (extending to the medial orbitofrontal cortex, frontal pole, and anterior cingulate cortex) was

Table 1
Effects of age on cortical thickness and subcortical volumes

Age-related reduction in cortical thickness				
Cortical clusters	Side	Cluster size (vertex)	Peak coordinates (Talairach)	*p*-Value
Precentral gyrus	L	93,314	−37 −18 64	0.0001
Inferior temporal gyrus	L	1576	−47 −58 −8	0.0001
Fusiform gyrus	L	1415	−35 −41 −11	0.0005
Superior parietal lobule	R	73,664	31 −48 44	0.0001
Postcentral gyrus	R	1031	30 −32 69	0.0063
Age-related reduction in subcortical volumes				
Subcortical structures	Side		*r*	$p_{FDR\text{-}corr}$
Thalamus	L		−0.54	<0.0001
	R		−0.55	<0.0001
Caudate nucleus	L		−0.58	<0.0001
	R		−0.60	0.0004
Putamen	L		−0.41	0.003
	R		−0.34	0.02
Accumbens nucleus	L		−0.36	0.01
	R		−0.46	0.001

Key: FDR, false discovery rate; L, left; R, right.

associated with higher REM sleep delta power in all but the frontal derivations (Table 2). Greater cortical thickness in the left lateral division of the orbitofrontal cortex and the right rostral division of the anterior cingulate cortex was also associated with higher REM sleep delta power in central derivations. Moreover, cortical thickness in the right superior temporal gyrus (extending to the insular and middle temporal cortices, as well as in the entorhinal cortex, parahippocampal and fusiform gyri) was positively associated with REM sleep delta power in parietal derivations. By contrast, lesser cortical thickness in the left lateral orbitofrontal cortex (extending to the superior frontal gyrus, frontal pole, and anterior cingulate cortex) was associated with higher REM sleep alpha power in frontal and central derivations. Lesser cortical thickness in the left insular cortex and in the right superior parietal gyrus was linked to higher REM sleep frontal alpha power, whereas lesser cortical thickness in the left superior frontal gyrus was associated with higher REM sleep central alpha power.

3.4.2. NREM sleep

In all subjects (independently of age and sex), greater cortical thickness in the left medial orbitofrontal cortex (extending to the superior frontal gyrus, frontal pole, and lateral orbitofrontal, and anterior cingulate cortices) was significantly associated with higher NREM sleep delta power in central derivations (Table 2). By contrast, lesser cortical thickness in the right lateral occipital cortex was associated with higher NREM sleep theta power in occipital derivations. Lesser cortical thickness in the left rostral division of the anterior cingulate cortex was also linked to higher NREM sleep alpha power in central derivations.

No significant relationship was found between REM or NREM sleep EEG and any subcortical volumes (FDR corrected $p' < 0.05$), and therefore, only cortical thickness clusters were subsequently included in mediation analyses.

3.5. Mediation modeling

We first computed conjunction analyses to identify, among all significant cortical thickness clusters, specific brain areas which were jointly associated with (1) age and (2) sleep EEG (after controlling for the effects of age and sex). Results are depicted in Fig. 2. Most cortical regions which showed significant associations with REM or NREM sleep EEG (independent of age and sex) also showed significant age-related thinning. Therefore, the reader is referred to Table 2 for cluster labeling and peak coordinates.

Given that age was associated with both sleep EEG and cortical thickness (similar regions linked to sleep EEG), we next sought to determine whether sleep EEG differences with age are driven by modifications in cortical integrity. To do so, we performed simple mediation analyses (see Supplementary Fig.1). Parameters estimates of each path analysis are detailed in Table 3.

3.5.1. REM sleep

We found that cortical thinning in bilateral superior frontal regions significantly mediated the effects of age on REM sleep EEG delta power (temporal, parietal, and occipital derivations; Table 3 and Fig. 2A–C). In addition, cortical thinning in the right superior temporal regions also significantly explained age-related reductions in parietal delta power during REM sleep (Table 3 and Fig. 2B).

3.5.2. NREM sleep

Similarly to what was found in REM sleep, age-related thinning in the left superior frontal gyrus significantly mediated the effect of age on NREM sleep central delta power (Table 3 and Fig. 2). Increased NREM sleep occipital theta power with age was also significantly mediated by the age-related thinning in the right lateral occipital cortex (Table 3 and Fig. 2D). However, age differences in NREM sleep occipital theta power were still significant when the right lateral

Table 2
Neuronal correlates of REM and NREM sleep EEG activity in adults

Cortical clusters	Side	Cluster size (vertex)	Peak coordinates (Talairach)	*p*-Value
REM sleep				
Delta: central				
Superior frontal gyrus	L	4179	−7 34 50	0.005
Lateral orbitofrontal cortex	L	5368	−26 24 −6	0.007
Rostral anterior cingulate cortex	R	4938	8 37 −4	0.002
Delta: temporal				
Superior frontal gyrus	L	4628	−13 53 3	0.002
	R	5806	13 54 28	0.0004
Delta: parietal				
Superior frontal gyrus	L	4261	−13 53 3	0.003
	R	5543	13 54 28	0.0007
Superior temporal gyrus	R	5862	49 −6 12	0.002
Delta: occipital				
Superior frontal gyrus	L	4465	−13 53 3	0.004
Alpha: frontal				
Insular cortex	L	9349	37 −13 2	0.0001
Lateral orbitofrontal cortex	L	21,425	−26 24 −6	0.0001
Superior parietal gyrus	R	9395	31 −48 44	0.0002
Alpha: central				
Superior frontal gyrus	L	3519	−13 53 3	0.01
Lateral orbitofrontal cortex	L	9380	−26 24 −6	0.0002
NREM sleep				
Delta: central				
Medial orbitofrontal cortex	L	4545	−13 53 3	0.004
Theta: occipital				
Lateral occipital cortex	R	3754	26 −95 −14	0.006
Alpha: central				
Rostral anterior cingulate cortex	L	4043	−13 53 3	0.008

Cortical regions showing significant relationships with sleep EEG activity, independent of age and sex ($p < 0.05$ corrected for multiple comparisons using a Monte Carlo simulation).
Key: EEG, electroencephalography; NREM, nonrapid eye movement; REM, rapid eye movement.

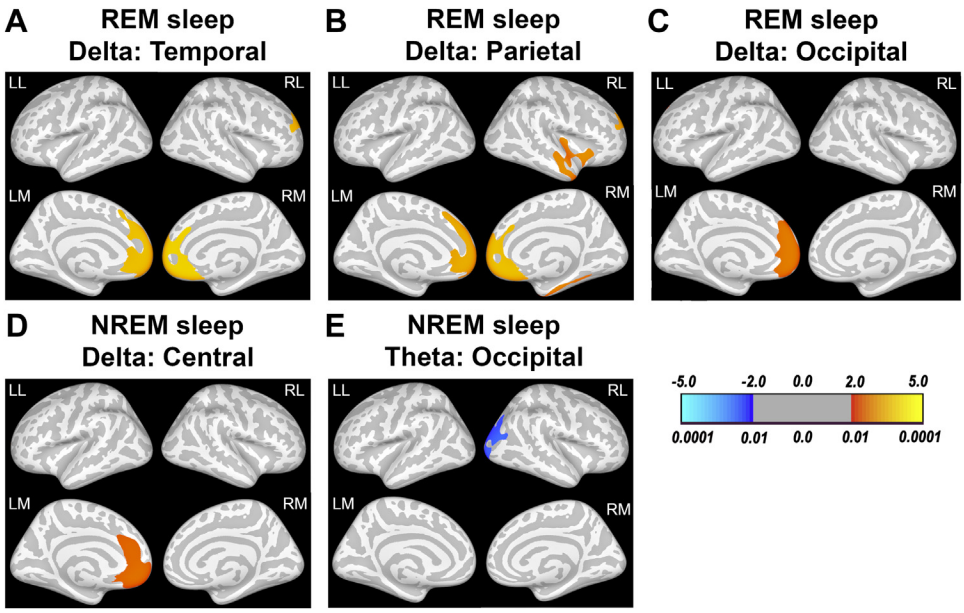

Fig. 2. Associations of REM and NREM sleep EEG with cortical thickness. Each panel shows cortical thickness clusters that are statistically correlated with sleep EEG spectral power in specific derivations (controlling for age and sex). (A) REM sleep delta power in temporal derivations; (B) REM sleep delta power in parietal derivations; (C) REM sleep delta power in occipital derivations; (D) NREM sleep delta power in central derivations; and (E) NREM sleep theta power in occipital derivations. Colors displayed are corrected *p*-values (Monte Carlo simulation): upper values are represented as −log10(p), ranging from −2 to −5 and 2 to 5, and lower values are their corresponding classical *p*-values, ranging from $p < 0.0001$ and $p < 0.01$. Hot colors represent the extent of the positive correlation between EEG and cortical thickness, while cold colors represent the extent of negative relationship between EEG and cortical thickness. Abbreviations: EEG, electroencephalography; LL, left lateral view; RL, right lateral view; LM, left medial view; RM, right medial view. (For interpretation of the references to color in this figure legend, the reader is referred to the Web version of this article.)

occipital cluster was entered in the model, indicating that other factors also contribute to age group differences (Table 3 and Fig. 2E).

3.6. Interstate conjunction analysis

To delineate further the core frontal substrate mediating age-related modifications in REM and NREM sleep relative delta power, we performed a conjunction analysis by calculating the intersection of the 4 contrast maps representing the associations between cortical thickness and REM (temporal, parietal, and occipital delta) and NREM (central delta) sleep spectral power. As depicted in Fig. 3, the resulting cluster is located in the left superior frontal gyrus, spreading to the rostral anterior cingulate and medial orbitofrontal cortices (1779 vertices).

3.7. Exploratory analyses of EEG during wakefulness after sleep onset

To explore whether our results are specific to sleep, we performed preliminary analyses in a subgroup of subjects from our cohort (n = 49) for whom we could select at least 60 seconds of wakefulness across the night (wakefulness after sleep onset, WASO). Results are detailed in Supplementary Data 1. Obviously, the use of WASO is not standard when analyzing resting-state EEG,

Table 3
Mediation results for REM and NREM sleep relative EEG power

Region	Parameter estimates				
	Path a	Path b	Path c'	Indirect effect (95% CI)	Partially standardized effect size (95% CI)
Total effect of age on REM sleep temporal delta (path c): $b = -6.80$, $p = 0.0005$					
L superior frontal	$b = -0.20$, $p < 0.001$	$b = 26.73$, $p < 0.001$	$b = -1.44$, $p = 0.51$	$b = -5.36$ (−8.31 to 2.90)	0.70 (0.38 to 1.05)
R superior frontal	$b = -0.17$, $p < 0.001$	$b = 33.23$, $p < 0.001$	$b = -1.01$, $p = 0.63$	$b = -5.80$ (−8.89 to 3.26)	0.75 (0.44 to 1.06)
Total effect of age on REM sleep parietal delta (path c): $b = -5.48$, $p = 0.005$					
L superior frontal	$b = -0.20$, $p < 0.001$	$b = 28.85$, $p < 0.001$	$b = 0.31$, $p = 0.89$	$b = -5.79$ (−8.96 to 3.13)	0.76 (0.42 to1.10)
R superior frontal	$b = -0.21$, $p < 0.001$	$b = 30.79$, $p < 0.001$	$b = 0.88$, $p = 0.70$	$b = -6.35$ (−10.12 to 3.34)	0.84 (0.46 to 1.21)
R superior temporal	$b = -0.17$, $p < 0.001$	$b = 36.19$, $p < 0.001$	$b = 0.72$, $p = 0.72$	$b = -6.20$ (−9.52 to 3.57)	0.81 (0.51 to 1.12)
Total effect of age on REM sleep occipital delta (path c): $b = -6.75$, $p = 0.0003$					
L superior frontal	$b = -0.21$, $p < 0.001$	$b = 26.70$, $p < 0.001$	$b = -1.27$, $p = 0.56$	$b = -5.48$ (−8.81 to 2.76)	0.74 (0.38 to 1.08)
Total effect of age on NREM sleep relative central delta (path c): $b = -4.76$, $p = 0.0004$					
L superior frontal	$b = -0.21$, $p < 0.001$	$b = 15.22$, $p = 0.02$	$b = -1.55$, $p = 0.39$	$b = -3.21$ (−5.87 to 1.00)	0.60 (0.18 to 1.00)
Total effect of age on NREM sleep relative occipital theta (path c): $b = 6.09$, $p < 0.001$					
R lateral occipital	$b = -0.12$, $p < 0.001$	$b = -19.87$, $p < 0.001$	$b = 3.78$, $p = 0.003$	$b = 2.31$ (1.16 to 4.04)	0.44 (0.21 to 0.74)

The total effect of age on each sleep EEG variable (path c) represents the direct effects of age on sleep EEG (controlling for sex), without the inclusion of cortical thickness in the model. Path a = effect of age on cortical thickness; Path b = relationship between cortical thickness and sleep EEG (controlling for age); Path c' = relationship between age and sleep EEG (controlling for cortical thickness); Indirect effect = effect of age on sleep EEG through an initial effect on cortical thickness (paths a*b). Indirect effects are considered significant when the confidence interval does not include zero (mediation).
Key: CI, confidence interval; EEG, electroencephalography; REM, rapid eye movement; NREM, nonrapid eye movement.

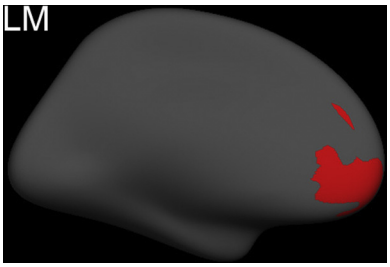

Fig. 3. Conjunction maps of delta power across REM and NREM sleep. Conjunction analysis of intersecting contrast maps for delta power during REM (temporal, parietal, and occipital derivations) and NREM sleep (central derivations; all independently corrected at $p < 0.05$ with a Monte Carlo simulation), showing a shared cortical thickness cluster located in the left superior frontal cortex, spreading to the rostral anterior cingulate and medial orbitofrontal cortices, and parts of the frontal pole. Abbreviations: REM, rapid eye movement; NREM, nonrapid eye movement; LM: left medial view.

but because no waking EEG was available from this cohort, we carefully selected EEG epochs free of any eye movements, muscle artifacts, or drowsiness related to sleep rhythms during WASO periods.

Briefly, we found that age effects on WASO EEG were similar to those of REM and NREM sleep (Supplementary Fig. 3). Compared with younger adults, older adults showed lower overall relative delta power, especially in frontal, central, and parietal regions. By contrast, older adults showed higher alpha power in the frontal region only, as well as higher beta power in central and temporal regions, as compared with younger adults.

In all subjects (independent of age and sex), greater cortical thickness in the left rostral middle frontal gyrus was significantly associated with higher WASO delta power in frontal derivations (Supplementary Table 2). Greater cortical thickness in the left lateral orbitofrontal cortex and in the right rostral middle frontal gyrus was also associated with higher WASO delta power in central derivations. Finally, cortical thickness in the right inferior frontal pars triangularis was positively associated with WASO delta power in parietal derivations. As for prior sleep EEG analyses, no significant relationship was found between WASO EEG spectral variables and subcortical volumes.

To explore whether age-related WASO EEG differences, especially for delta activity, can be statistically explained by modifications in cortical integrity, we performed the same mediation model as for sleep EEG (see Supplementary Table 3 for parameters estimates of each path analysis). Overall, we found that cortical thinning in medial orbitofrontal, middle frontal, and pars triangularis regions significantly mediated the effects of age on WASO EEG delta power (frontal, central, and parietal derivations; Supplementary Fig. 4A–C).

4. Discussion

Our findings support that REM sleep EEG activity can serve as a marker of cortical integrity in healthy adults. We also demonstrate that thinning of the medial frontal cortex significantly contributes to lower delta power during both REM and NREM sleep in healthy older adults.

4.1. Frontal cortical thinning statistically explains lower REM and NREM sleep delta in older adults

Our results indicate that the impact of cortical frontal thinning on delta activity goes beyond NREM sleep—it also drives changes in REM sleep. This suggests that common mechanisms are at play in the reduction of delta activity during REM and NREM sleep with age. Previous studies demonstrated that reduced prefrontal and frontal gray matter associated with aging might be responsible for disrupted NREM sleep delta activity (Dube et al., 2015; Mander et al., 2013; Varga et al., 2016). A study also showed that poor subjective sleep quality, particularly sleep efficiency (as measured subjectively by the Pittsburgh Sleep Quality Inventory) was associated with a greater rate of atrophy over time in similar brain areas (i.e., the bilateral medial superior frontal gyrus and cingulate cortex) (Sexton et al., 2014). Our results indicate that cortical thickness in the medial frontal areas and anterior cingulate cortices explains age-related lower delta power during both REM and NREM sleep.

With all their connections to and from other key areas of the brain, the medial frontal areas, and notably the anterior cingulate cortex, have been proposed as major hubs of the human encephalon (van den Heuvel and Sporns, 2013). Several studies have demonstrated their synchronizing role; during sleep, the medial frontal gyrus and the cingulate cortex facilitate the propagation of slow waves from anterior to posterior areas of the brain (Murphy et al., 2009), and during wakefulness, stimulation of the anterior cingulate cortex induces widespread synchronous activity mimicking EEG sleep K-complexes (Voysey et al., 2015). Although further studies are needed to ascertain more precisely the role of the superior frontal and anterior cingulate cortices in the initiation of large-scale neuronal synchrony, it is likely that these structures play a major role in sustaining low-frequency activity during REM and NREM sleep. With advancing age, the thinning of the superior frontal and anterior cingulate cortices may therefore compromise adequate low-frequency neuronal firing during sleep, leading to reduced delta activity as seen in our cohort of older adults.

By contrast to NREM sleep, frontal cortical thinning mediated the effects of age on REM sleep delta power in the posterior scalp derivations (i.e., temporal, parietal, and occipital). One would have expected the frontal cortical thickness to be linked to frontal delta power during REM sleep. Although older adults showed lower delta power in the frontal regions compared with younger ones, the most prominent age effects on delta power were observed in the temporal, parietal, and occipital regions. With aging, frontal cortical thinning may compromise the propagation of synchronous/low-frequency activity from the anterior brain areas toward the posterior regions during sleep. Further studies will be needed to determine whether this age-related reduction in REM sleep delta power reflects a disrupted distal and long-range EEG connectivity.

We performed exploratory EEG analyses of WASO as an extra step to better understand the mechanisms underlying age-related delta modifications. As discussed previously, the use of WASO is not standard when analyzing resting-state EEG, and may very well have a different spectral signature from standard waking EEG. Nevertheless, our exploratory analyses of EEG-cortical thickness relationships during WASO periods revealed some similarities but also some discrepancies with our sleep findings. Overall, there is a common frontal substrate mediating the effect of age on delta power across the 3 conscious states (WASO, REM, and NREM sleep). However, the clusters associated with age-related differences in delta power during WASO were located more laterally over the rostral middle frontal gyrus and inferior frontal gyrus, whereas for REM and NREM sleep delta power, the intersecting cluster was located more medially over the superior frontal and anterior cingulate cortices. Future studies will be needed to confirm these exploratory observations using larger data samples from standard resting-state wakefulness protocols in young and older healthy adults.

4.2. Relative delta power: a measure of neural synchronization in REM sleep?

Although REM sleep EEG does not have defined slow waves, prior work in rodents showed that slow waves do occur during REM sleep in localized cortical regions and layers (Funk et al., 2016). A recent study also showed local increases of delta power during REM sleep relative to wakefulness using high-density EEG (Baird et al., 2018). In addition, we show that relative delta power in REM and NREM sleep share similar brain substrates: significant positive relationships were observed between cortical thickness in the medial frontal regions and REM and NREM sleep delta power.

The amplitude of a surface EEG measure is not only dependent on the magnitude of individual current dipoles, but also on the degree of their temporal synchronization. Numerous studies suggest that a higher contribution of lower frequencies relative to higher frequencies is indicative of higher neuronal synchronization, and this has been shown not only in NREM sleep following sleep deprivation, but also during resting-state wakefulness and REM sleep EEG (Brunner et al., 1990; Ferreira et al., 2006; Marzano et al., 2007). Moreover, an increase in local field potential spectral power in the slow-theta range is observed following sleep deprivation in the awake animal and during NREM sleep (Vyazovskiy et al., 2009; Vyazovskiy and Harris, 2013). Importantly, these slow-theta local field potential waves are accompanied with enhanced OFF periods in populations of neurons during wake and NREM sleep, reflecting increased synchronization (Vyazovskiy et al., 2009; Vyazovskiy and Harris, 2013).

Our results indicate that the relative contribution of delta/low frequencies over higher frequencies during REM and NREM sleep is smaller in older adults compared with younger adults. The electrophysiological mechanisms underlying the effects of age on wake, REM, and NREM sleep EEG still need to be determined but might very well reflect lower neuronal synchronization during OFF periods.

4.3. An integrated perspective of the relationship between sleep EEG and frontal brain regions in normal and pathological aging

Our findings of reduced delta activity during REM sleep and WASO in healthy older as compared with young adults contrast with results found in pathological aging populations. Indeed, adults with age-related pathological or neurodegenerative conditions such mild cognitive impairment, Alzheimer's disease (AD), and Parkinson's disease (PD) show an opposite EEG pattern: as compared with healthy controls of similar age, they show EEG slowing characterized by greater delta and theta power and lower alpha and beta power during REM sleep and resting wakefulness (Babiloni et al., 2004; Brayet et al., 2014; Latreille et al., 2016; Petit et al., 1993). This REM sleep and wake EEG slowing has been hypothesized to be linked to the cholinergic dysfunction seen early on in the course of AD and PD. Because the cholinergic system constitutes an integral part of the reticular activating system, which serves to modulate EEG rhythms during sleep and wakefulness (Garcia-Rill, 2009), degeneration of this system in AD (basal forebrain cholinergic neurons) and PD (brainstem cholinergic pedunculopontine and tegmental neurons) is thought to contribute to EEG slowing (for more details, see Herholz et al., 2008; Latreille et al., 2016). By reducing its activating input to the cortex via thalamocortical projections, cell loss or abnormal activity within the ascending cholinergic systems may result in slower cortical rhythms during REM sleep and wakefulness. In addition to subcortical cholinergic dysfunction, widespread cortical atrophy may also disrupt the corticothalamic feedback loop, sustaining these slow firing rates and resultant low-frequency EEG activity.

Our results in healthy older adults suggest that the physiology of EEG changes with normal aging differ from pathological aging. In our cohort, although older individuals showed lower volume for several subcortical structures (thalamus, putamen, caudate, and accumbens nuclei), this age-related atrophy did no predict EEG differences. In the context of normal aging and in the absence of cognitive impairment, it is possible that the "relative" preservation of the subcortical structures may help maintain "good" functioning of the reticular activating system and thus prevent EEG slowing. On the cortical level, diminished frontal cortical integrity would however impair the neuron's ability to sustain low-frequency activity, resulting in reduced EEG delta power in older adults.

4.4. Limitations, future studies, and conclusion

Some limitations of this study must be mentioned. We acknowledge that the conclusions regarding our REM sleep results are based on more restricted EEG data samples as compared with NREM sleep, and that our findings are only generalizable to tonic REM sleep as we did not include phasic REM sleep. Yet, in a recent study, the comparison of delta activity during tonic and phasic REM sleep revealed no differences in power or in topography, suggesting that delta power during REM sleep is independent of the tonic or phasic phases (Baird et al., 2018). In addition, our study did not have sufficient statistical power to test whether the relationship between cortical thickness and sleep EEG differed between men and women. Future work using large cohorts of men and women will help to examine this possible interaction.

In conclusion, by investigating both REM and NREM sleep, we were able to disentangle the specificities and commonalities of each sleep state's association with cortical thickness integrity. Our findings demonstrate that impaired gray matter cortical integrity in medial anterior regions jointly contributes to the reduction of delta activity during REM and NREM sleep with aging. These results support the notion that sleep and its inherent EEG components can reflect cortical changes, and serve as a proxy of cortical integrity. Investigating sleep EEG in health and disease may therefore provide further insights about the integrity of the underlying cortical network, which may ultimately help target specific mechanisms to prevent the development of pathological processes.

Disclosure

The authors have no actual or potential conflicts of interest.

Acknowledgements

The authors would like to thank Sonia Frenette, RPSGT, for her help with data acquisition and analysis.

This work was supported by the Canadian Institutes of Health Research (CIHR) Grant 93733 (J.C.) and CIHR scholarship (V.L).

Appendix A. Supplementary data

Supplementary data associated with this article can be found, in the online version, at https://doi.org/10.1016/j.neurobiolaging.2018.12.012.

References

American Psychiatric Association, 2013. Diagnostic and statistical manual of mental disorders, fifth ed. (DSM-5). In: Diagnostic Stat. Man. Ment. Disord, fourth ed. TR. 280.

Babiloni, C., Binetti, G., Cassetta, E., Cerboneschi, D., Dal Forno, G., Del Percio, C., Ferreri, F., Ferri, R., Lanuzza, B., Miniussi, C., Moretti, D.V., Nobili, F., Pascual-Marqui, R.D., Rodriguez, G., Romani, G.L., Salinari, S., Tecchio, F., Vitali, P., Zanetti, O., Zappasodi, F., Rossini, P.M., 2004. Mapping distributed sources of cortical rhythms in mild Alzheimer's disease. A multicentric EEG study. Neuroimage 22, 57–67.

Baird, B., Castelnovo, A., Riedner, B.A., Lutz, A., Ferrarelli, F., Boly, M., Davidson, R.J., Tononi, G., 2018. Human rapid eye movement sleep shows local increases in low-frequency oscillations and global decreases in high-frequency oscillations compared to resting wakefulness. eNeuro 5. https://doi.org/10.1523/ENEURO.0293-18.2018.

Beck, A.T., Ward, C.H., Mendelson, M., Mock, J., Erbaugh, J., 1961. An inventory for measuring depression. Arch. Gen. Psychiatry 4, 561–571.

Benjamini, Y., Hochberg, Y., 1995. Controlling the false discovery rate: a practical and powerful approach to multiple testing. J. R. Stat. Soc. B. 57, 289–300. https://doi.org/10.2307/2346101.

Bolduc, C., Daoust, A.M., Limoges, É., Braun, C.M.J., Godbout, R., 2003. Hemispheric lateralization of the EEG during wakefulness and REM sleep in young healthy adults. Brain Cogn. 53, 193–196.

Brayet, P., Petit, D., Frauscher, B., Gagnon, J.F., Gosselin, N., Gagnon, K., Rouleau, I., Montplaisir, J., 2014. Quantitative EEG of rapid-eye-movement sleep: a marker of amnestic mild cognitive impairment. Clin. EEG. Neurosci. 47, 134–141.

Brunner, D., Vasko, R., Detka, C., Monahan, J., Reynolds, C.I., Kupfer, D., 1996. Muscle artifacts in the sleep EEG: automated detection and effect on all-night EEG power spectra. J. Sleep Res. 5, 155–164.

Brunner, D.P., Dijk, D.J., Tobler, I., Borbély, A.A., 1990. Effect of partial sleep deprivation on sleep stages and EEG power spectra: evidence for non-REM and REM sleep homeostasis. Electroencephalogr. Clin. Neurophysiol. 75, 492–499.

Carrier, J., Viens, I., Poirier, G., Robillard, R., Lafortune, M., Vandewalle, G., Martin, N., Barakat, M., Paquet, J., Filipini, D., 2011. Sleep slow wave changes during the middle years of life. Eur. J. Neurosci. 33, 758–766.

Dang-Vu, T.T., Desseilles, M., Laureys, S., Degueldre, C., Perrin, F., Phillips, C., Maquet, P., Peigneux, P., 2005. Cerebral correlates of delta waves during non-REM sleep revisited. Neuroimage 28, 14–21.

Desikan, R.S., Ségonne, F., Fischl, B., Quinn, B.T., Dickerson, B.C., Blacker, D., Buckner, R.L., Dale, A.M., Maguire, R.P., Hyman, B.T., Albert, M.S., Killiany, R.J., 2006. An automated labeling system for subdividing the human cerebral cortex on MRI scans into gyral based regions of interest. Neuroimage 31, 968–980.

Dube, J., Lafortune, M., Bedetti, C., Bouchard, M., Gagnon, J.F., Doyon, J., Evans, A.C., Lina, J.-M., Carrier, J., 2015. Cortical thinning explains changes in sleep slow waves during adulthood. J. Neurosci. 35, 7795–7807.

Ferreira, C., Deslandes, A., Moraes, H., Cagy, M.M., Pompeu, F., Basile, L.F., Piedade, R., Ribeiro, P., 2006. Electroencephalographic changes after one night of sleep deprivation. Arq. Neuropsiquiatr. 64, 388–393.

Fischl, B., Dale, A.M., 2000. Measuring the thickness of the human cerebral cortex from magnetic resonance images. Proc. Natl. Acad. Sci. 97, 11050–11055.

Fjell, A.M., Walhovd, K.B., 2010. Structural brain changes in aging: courses, causes and cognitive consequences. Rev. Neurosci. 21, 187–221.

Funk, C.M., Honjoh, S., Rodriguez, A.V., Cirelli, C., Tononi, G., 2016. Local slow waves in superficial layers of primary cortical areas during REM sleep. Curr. Biol. 26, 396–403.

Garcia-Rill, E., 2009. Reticular activating system. In: Squire, L. (Ed.), Encyclopedia of Neuroscience. Elsevier, Oxford, England, pp. 137–143. https://doi.org/10.1016/B978-008045046-9.01767-8.

Goodro, M., Sameti, M., Patenaude, B., Fein, G., 2012. Age effect on subcortical structures in healthy adults. Psychiatry Res. 203, 38–45.

Hayes, A., 2013. Introduction to Mediation, Moderation, and Conditional Process Analysis. The Guilford Press, New York, NY, pp. 3–4.

Herholz, K., Weisenbach, S., Kalbe, E., 2008. Deficits of the cholinergic system in early AD. Neuropsychologia 46, 1642–1647.

Hofle, N., Paus, T., Reutens, D., Fiset, P., Gotman, J., Evans, A.C., Jones, B.E., 1997. Regional cerebral blood flow changes as a function of delta and spindle activity during slow wave sleep in humans. J. Neurosci. 17, 4800–4808.

Iber, C., Ancoli-Israel, S., Chesson, A., Quan, S., 2007. The AASM Manual for the Scoring of Sleep and Associates Events: Rules, Terminology and Technical Specifications. Sleep, Rochester.

Krishnan, G.P., Chauvette, S., Shamie, I., Soltani, S., Timofeev, I., Cash, S.S., Halgren, E., Bazhenov, M., 2016. Cellular and neurochemical basis of sleep stages in the thalamocortical network. Elife 5, 1–29.

Landolt, H.P., Borbély, a a, 2001. Age-dependent changes in sleep EEG topography. Clin. Neurophysiol. 112, 369–377.

Latreille, V., Carrier, J., Gaudet-Fex, B., Rodrigues-Brazète, J., Panisset, M., Chouinard, S., Postuma, R.B., Gagnon, J.-F., 2016. Electroencephalographic prodromal markers of dementia across conscious states in Parkinson's disease. Brain 139 (Pt 4), 1189–1199.

Lemaitre, H., Goldman, A.L., Sambataro, F., Verchinski, B.A., Meyer-Lindenberg, A., Weinberger, D.R., Mattay, V.S., 2012. Normal age-related brain morphometric changes: nonuniformity across cortical thickness, surface area and gray matter volume? Neurobiol. Aging 33, 617.e1–617.e9.

Léveillé, C., Barbeau, E.B., Bolduc, C., Limoges, E., Berthiaume, C., Chevrier, Elyse, Mottron, L., Godbout, R., 2010. Enhanced connectivity between visual cortex and other regions of the brain in autism: A REM sleep EEG coherence study. Autism Res. 3, 280–285.

Long, X., Liao, W., Jiang, C., Liang, D., Qiu, B., Zhang, L., 2012. Healthy aging. an automatic analysis of global and regional morphological alterations of human brain. Acad. Radiol. 19, 785–793.

Luca, G., Haba Rubio, J., Andries, D., Tobback, N., Vollenweider, P., Waeber, G., Marques Vidal, P., Preisig, M., Heinzer, R., Tafti, M., 2015. Age and gender variations of sleep in subjects without sleep disorders. Ann. Med. 47, 482–491.

Mander, B.A., Marks, S.M., Vogel, J.W., Rao, V., Lu, B., Saletin, M., Ancoli-israel, S., Jagust, W.J., Walker, M.P., 2016. β-amyloid disrupts human NREM slow waves and related hippocampus-dependent memory consolidation. Nat. Neurosci. 18, 1051–1057.

Mander, B.A., Rao, V., Lu, B., Saletin, J.M., Lindquist, J.R., Ancoli-Israel, S., Jagust, W., Walker, M.P., 2013. Prefrontal atrophy, disrupted NREM slow waves and impaired hippocampal-dependent memory in aging. Nat. Neurosci. 16, 357–364.

Mander, B.A., Winer, J.R., Walker, M.P., 2017. Sleep and human aging. Neuron 94, 19–36.

Maquet, P., 2000. Functional neuroimaging of normal human sleep by positron emission tomography. J. Sleep Res. 9, 207–231.

Maquet, P., Degueldre, C., Delfiore, G., Aerts, J., Péters, J.-M., Luxen, A., Franck, G., 1997. Functional neuroanatomy of human slow wave sleep. J. Neurosci. 17, 2807–2812.

Maquet, P., Peters, J.M., Aerts, J., Delfiore, G., Degueldre, C., Luxen, A., Franck, G., 1996. Functional neuroanatomy of human rapid-eye-movement sleep and dreaming. Nature 383, 163–166.

Martin, N., Lafortune, M., Godbout, J., Barakat, M., Robillard, R., Poirier, G., Bastien, C., Carrier, J., 2013. Topography of age-related changes in sleep spindles. Neurobiol. Aging 34, 468–476.

Marzano, C., Fratello, F., Moroni, F., Pellicciari, M.C., Curcio, G., Ferrara, M., Ferlazzo, F., De Gennaro, L., 2007. Slow eye movements and subjective estimates of sleepiness predict EEG power changes during sleep deprivation. Sleep 30, 610–616.

Morisson, F., Lavigne, G., Petit, D., Nielsen, T.A., Malo, J., Montplaisir, J., 1998. Spectral analysis of wakefulness and REM sleep EEG in patients with sleep apnoea syndrome. Eur. Respir. J. 11, 1135–1140.

Murphy, M., Riedner, B.A., Huber, R., Massimini, M., Ferrarelli, F., Tononi, G., 2009. Source modeling sleep slow waves. Proc. Natl. Acad. Sci. 106, 1608–1613.

Nofzinger, E.A., Buysse, D.J., Miewald, J.M., Meltzer, C.C., Price, J.C., Sembrat, R.C., Ombao, H., Reynolds, C.F., Monk, T.H., Hall, M., Kupfer, D.J., Moore, R.Y., 2002. Human regional cerebral glucose metabolism during non-rapid eye movement sleep in relation to waking. Brain 125, 1105–1115.

Patenaude, B., Smith, S.M., Kennedy, D.N., Jenkinson, M., 2011. A Bayesian model of shape and appearance for subcortical brain segmentation. Neuroimage 56, 907–922.

Petit, D., Lorrain, D., Gauthier, S., Montplaisir, J., 1993. Regional spectral analysis of the REM sleep EEG in mild to moderate Alzheimer's disease. Neurobiol. Aging 14, 141–145.

Sexton, C.E., Storsve, A.B., Walhovd, K.B., Johansen-Berg, H., Fjell, A.M., 2014. Poor sleep quality is associated with increased cortical atrophy in community-dwelling adults. Neurology 83, 967–973.

Shaw, M.E., Abhayaratna, W.P., Sachdev, P.S., Anstey, K.J., Cherbuin, N., 2016. Cortical thinning at midlife: the PATH through life study. Brain Topogr 29, 875–884.

van den Heuvel, M.P., Sporns, O., 2013. Network hubs in the human brain. Trends Cogn. Sci. 17, 683–696.

Varga, A.W., Ducca, E.L., Kishi, A., Fischer, E., Parekh, A., Koushyk, V., Yau, P.L., Gumb, T., Leibert, D.P., Wohlleber, M.E., Burschtin, O.E., Convit, A., Rapoport, D.M., Osorio, R.S., Ayappa, I., 2016. Effects of aging on slow-wave sleep dynamics and human spatial navigational memory consolidation. Neurobiol. Aging 42, 142–149.

Voysey, Z., Martín-López, D., Jiménez-Jiménez, D., Selway, R.P., Alarcón, G., Valentín, A., 2015. Electrical stimulation of the anterior cingulate gyrus induces responses similar to k-complexes in awake humans. Brain Stimul 8, 881–890.

Vyazovskiy, V.V., Harris, K.D., 2013. Sleep and the single neuron: The role of global slow oscillations in individual cell rest. Nat. Rev. Neurosci. 14, 443–451.

Vyazovskiy, V.V., Olcese, U., Lazimy, Y.M., Faraguna, U., Esser, S.K., Williams, J.C., Cirelli, C., Tononi, G., 2009. Cortical firing and sleep homeostasis. Neuron 63, 865–878.